

A Novel Trajectory Planning Method for a Robotic Fish

Michail Makrodimitris, *Student Member IEEE*, Kostas Nanos
and Evangelos Papadopoulos, *Senior Member IEEE*

Abstract—Recently, there has been a growing interest in biomimetic underwater vehicles. Although a lot of research has been conducted in the area of dynamics and kinematics of robotic fish, most of the approaches solve the inverse problem by finding the required force the caudal fin should produce, in order for the robotic fish to follow a trajectory. Others use predefined undulatory body motions which usually approximate paths of simple planar geometrical shapes, such as circles and straight lines. The attempts cannot conclude a priori if a robotic fish can actually follow the given trajectory. More importantly, they cannot derive caudal fin trajectories that will ensure that the fish will follow a given planar trajectory. In this paper we present a novel and universal methodology for finding how the caudal fin of a robotic fish should move, so that the robotic fish follows any planar trajectory. Also, we identify the sufficient conditions, which must be satisfied to predict a priori, whether the robotic fish is able to follow a given trajectory. To the best of the knowledge of the authors, this is the first time that such a methodology is presented. Finally, experimental results are provided, showing the merits of the developed method.

I. INTRODUCTION

Achieving accurate motion control in underwater robotics is especially important and has been a subject of extensive research in the robotics field spanning the last decade. The nonlinear nature of the hydrodynamic forces, which act on the robotic fish (See Fig. 1), combined with the fact that these systems are subject to nonholonomic constraints and underactuation, make the research of trajectory tracking quite challenging. Trajectory tracking is a motion control problem associated with the design of controllers that force a vehicle to follow a time parameterized geometric path. The classical approach for trajectory-tracking of underactuated robotic fish utilizes kinematic and dynamic models. One of the first attempts to connect the required forces with the generalized coordinates and their derivatives of a robotic fish were presented in [1]. No simulations or experiments were carried out. In [2], the authors utilize simple geometrical elements (circles and lines) to find the shortest feasible path between two points, without experimental evaluation. In this case some form of discontinuity can not be avoided. Inverse dynamics control methods, which compute the forces rather than the caudal fin profile in order to follow a trajectory, are presented in [3], [4]. There is extensive literature regarding Lighthill's theory, an inverse dynamic control method based

on non-linear state function models including hydrodynamics, which improves tracking performance by selecting the appropriate body undulatory wave function for the robotic fish propulsion, e.g [5], [6]. In [7], the authors integrate the Theodorsen function, in order to compute the thrust force. In [8], the well-known Joukowski solution is employed. In order to have accurate trajectory tracking, the authors use an extreme seeking algorithm. Although their results are satisfactory, the complexity of the algorithms make the implementation in low-cost hardware dubious.

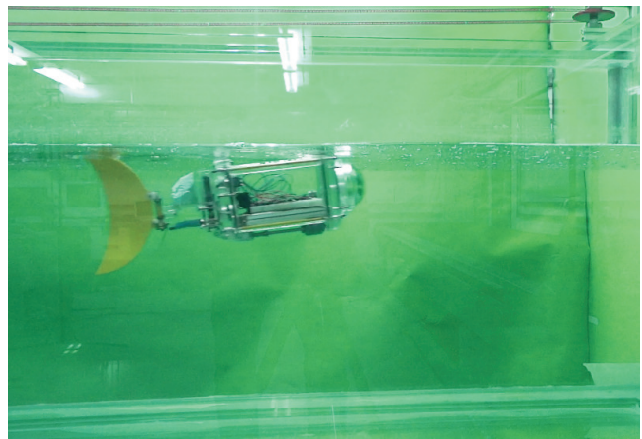


Fig. 1. The CSL Robotic Fish in a test tank.

Other researchers try to use simple approaches such as finding a relation between offset angle and radius which the robotic fish should follow [9], and transfer functions which have as input the desired path angle and as output the angle rate [10]. The latter suffers from large overshoots in open loop and needs a controller. Modern approaches regarding trajectory planning of robotic fish involve the approximation of thrust force with a nondimensional coefficient of thrust [11], central pattern generators [12], fuzzy logic controllers [13], where experimental data shows maximum error of about 20% for the tail, requiring more inputs, as well as neural networks [14], where discontinuities in the trajectory of the center of the fish are observed.

The main contribution of this paper is the derivation of the required motion of the caudal fin in order for the fish to follow any feasible desired planar trajectory, exploiting the dynamics of the CSL robot fish (see Fig.1). In addition, the necessary conditions are given in order to predict a priori if the trajectory can be followed.

M. Makrodimitris (e-mail: mmakro@gmail.com), K. Nanos (e-mail: nanos.kostas@gmail.com) and E. Papadopoulos (e-mail: egpado@central.ntua.gr, tel: +30 210-772-1440) are with the School of Mechanical Engineering, National Technical University of Athens, 15780 Athens, Greece.

II. ROBOT FISH DYNAMICS

In this section, the dynamical model of the robotic fish is developed, to be investigated by simulations and experiments. The CSL fish belongs to the Carangiform class and therefore it consists of two connected parts: the main body and the caudal fin (see Fig. 2). Three coordinate frames are defined: (a) The inertial coordinate frame with \hat{X}, \hat{Y} unit vectors, (b) the main body coordinate frame with \hat{x}, \hat{y} unit vectors and (c) the caudal fin coordinate frame with \hat{k}, \hat{i} unit vectors.

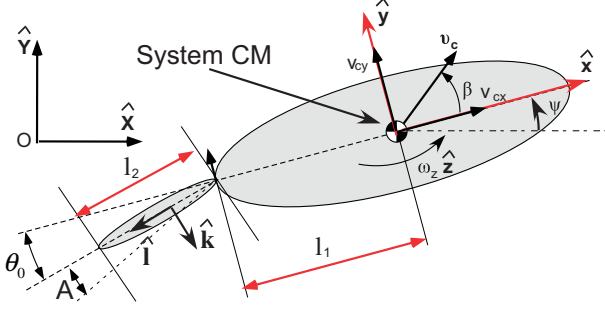


Fig. 2. Robotic Fish Model

Since the caudal fin's mass is negligible in comparison to the main body, the following assumptions are made: (a) the fish consists of the main body only, but the hydrodynamic forces acting on the caudal fin, are referenced in the main body coordinate frame, and (b) the center of mass (CM) of the two bodies (main body and caudal fin) and the CM of the main body coincide, since the caudal fin mass contributes little to the overall mass. It is also assumed that the origin of the main body-fixed system coincides with the center of gravity and the shape of the caudal fin is rectangular. Thus, based on [15], the equations of motion for a 3D rigid body moving on a plane, expressed in the fish body-fixed frame, are given by:

$$\begin{aligned} m_b (\dot{\mathbf{v}}_c + (\boldsymbol{\omega}_z \hat{\mathbf{z}}) \times \mathbf{v}_c) &= \mathbf{f}_c \\ \mathbf{I}_c (\dot{\boldsymbol{\omega}}_z \hat{\mathbf{z}}) + (\boldsymbol{\omega}_z \hat{\mathbf{z}}) \times \mathbf{I}_c (\boldsymbol{\omega}_z \hat{\mathbf{z}}) &= \mathbf{M}_c \end{aligned} \quad (1)$$

where $\mathbf{v}_c = [v_{cx} \ v_{cy}]^T$ is the linear velocity [m/s], $\dot{\mathbf{v}}_c$ is the linear acceleration [m/s²] of the fish CM, $\boldsymbol{\omega}_z, \dot{\boldsymbol{\omega}}_z$ are its angular acceleration [rad/s²] and angular velocity [rad/s], $\mathbf{f}_c, \mathbf{M}_c$ are the sum of forces [N] and moments [Nm] which act on the rigid body, and m_b, \mathbf{I}_c are the mass [kg] and the inertia tensor of the rigid body.

Moreover, since an accelerating or decelerating body must move (or deflect) some volume of surrounding fluid as it moves through, an added mass, namely the inertia added to a system, must be included, too. Then, for planar motions, the following set of equations for each axis results:

$$\begin{aligned} (m_b - X_{\dot{v}_{cx}}) \dot{v}_{cx} &= (m_b - Y_{\dot{v}_{cy}}) v_{cy} \omega_z + f_x \\ (m_b - Y_{\dot{v}_{cy}}) \dot{v}_{cy} &= -(m_b - X_{\dot{v}_{cx}}) v_{cx} \omega_z + f_y \\ (\mathbf{I}_c - N_{\dot{\omega}_z}) \dot{\omega}_z &= (Y_{\dot{v}_{cy}} - X_{\dot{v}_{cx}}) v_{cx} v_{cy} + \tau_z \end{aligned} \quad (2)$$

where $X_{\dot{v}_{cx}}, Y_{\dot{v}_{cy}}, N_{\dot{\omega}_z}$ are the added masses, f_x, f_y [N] and τ_z [Nm] are the forces and moment which act in x, y and z axis

respectively, and v_{cx}, v_{cy} are the surge and sway velocities [m/s] of the main body of the robotic fish.

There is a number of ways to compute the added masses ($X_{\dot{v}_{cx}}, Y_{\dot{v}_{cy}}, N_{\dot{\omega}_z}$), e.g Lamb's factors, slender body theory, [16] etc. In this paper, the added mass values are taken as 10% of the body mass in every direction of motion.

The computation of the forces f_x, f_y and the moment τ_z is very important. These forces and moment are due to the lift F_L and drag forces F_D , drag moment M_D , which act on the main body, as well as to the thrust forces F_{tx}, F_{ty} [N] and moment M_{tz} [Nm] which are produced by the oscillatory motion of the tail. All the above variables are expressed in the main body coordinate frame. The drag and lift forces which act on the caudal fin, are omitted as they are very small compared to the corresponding forces of the main body.

Under the above assumptions, the form of the forces f_x, f_y and the moment τ_z is simplified to:

$$\begin{aligned} f_x &= F_{tx} - F_D \cos \beta + F_L \sin \beta \\ f_y &= F_{ty} - F_D \sin \beta - F_L \cos \beta \\ \tau_z &= M_{tz} + M_D \end{aligned} \quad (3)$$

where $\beta = \arctan(v_{cy}/v_{cx})$ is the angle of attack [rad] of the fish main body (See Fig.2). Common models which describe these forces and moment in the literature are, [17]:

$$\begin{aligned} F_D &= 0.5 \rho \|\mathbf{v}_c\|^2 S_A C_D \\ F_L &= 0.5 \rho \|\mathbf{v}_c\|^2 S_A C_L \beta \\ M_D &= -K_D \omega_z |\omega_z| \end{aligned} \quad (4)$$

where $\|\cdot\|$ denotes the Euclidean norm of the vector (\cdot) and $|\omega_z|$ denotes the absolute value of ω_z . C_D is the drag force coefficient of the main body, C_L is its lift force coefficient, K_D the drag moment coefficient of the main body and ρ the density of the water [kg/m³]. The term S_A defines the reference surface area of the fish [m²]. This area is perpendicular to the velocity of the main body of the robot fish, thus it is variable. Since the yaw angles of the fish are small, the assumption that this area changes very little is reasonable, and therefore the surface area S_A is taken as constant.

For the same reason, the parameters C_D and K_D are considered constant, too, even though it is known that they depend on the attack angle β . To evaluate the thrust forces and moment F_{tx}, F_{ty} and M_{tz} which are produced by the caudal fin and are the forces which propel the fish, the Lighthill's large-amplitude elongated-body theory is used, [18], [19].

Based on hydrodynamic simulations and the fact that velocities perpendicular to caudal fin are much larger than velocities parallel to it, it is assumed that only a force, perpendicular to the caudal fin is applied to it. The force per unit area of the caudal fin \mathbf{f}_t^* [N/m²] is approximated for small angles as:

$$\mathbf{f}_t^* = -m^* \ddot{\theta} \hat{\mathbf{k}} \quad (5)$$

where m^* denotes the virtual mass per unit length [kg/m] and can be approximated by $\frac{1}{4} \pi \rho d^2$, d is the height of the

cross-section of the tail [18] and $\ddot{\theta}$ is the angular acceleration of the caudal fin [rad/s^2].

The caudal fin is activated by a DC servo controlled by a simple PD controller, commanded so that the caudal fin deflection angle $\theta(t)$ [rad] follows:

$$\theta(t) = \theta_0 + A \sin(\omega t). \quad (6)$$

where θ_0 the offset angle [rad], A the amplitude [rad], t the time [s] and ω the angular frequency [rad/s] of the caudal fin. The tail deflection angles must be subject to bounds so that the phenomenon of stall does not occur.

Based on previous assumptions and (5), the resulting equations, which give the thrust forces F_{t_x}, F_{t_y} , caused by the movement of the caudal fin, expressed in the main body coordinate frame (\hat{x}, \hat{y}) , are:

$$F_{t_x} = -m^* \ddot{\theta} \frac{l_2^2}{2} \sin \theta \quad (7)$$

$$F_{t_y} = m^* \ddot{\theta} \frac{l_2^2}{2} \cos \theta \quad (8)$$

where l_2 is the caudal fin length, (see Fig. 2).

The magnitude of the moment caused by the tail oscillation and expressed in the body-fixed frame, is given by:

$$M_{t_z} = \int_0^{l_2} \|\mathbf{r}_c \times \mathbf{f}_t\| dl \quad (9)$$

where dl is an elementary part of the caudal fin and \mathbf{f}_t is the force acting per unit length on the caudal fin because of its motion in the surrounding fluid:

$$\mathbf{f}_t = \int_0^{l_2} \mathbf{f}_t^* dl = - \int_0^{l_2} m^* \ddot{\theta} \hat{\mathbf{k}} dl \quad (10)$$

and \mathbf{r}_c is the vector from the CM of the main body to an arbitrary point of the tail, measured from the main body coordinate frame:

$$\mathbf{r}_c = (-l_1 - l \cos \theta) \hat{\mathbf{x}} - l \sin \theta \hat{\mathbf{y}} \quad (11)$$

where l_1 [m] is the distance between the center of the mass of the main body to the tail joint (see Fig. 2), and l is the distance of the element dl from the joint. Evidently $0 \leq l \leq l_2$. After some algebraic manipulations we obtain:

$$M_{t_z} = -\frac{l_2^3}{3} m^* \ddot{\theta} - \frac{l_2^2}{2} m^* \ddot{\theta} l_1 \cos \theta \quad (12)$$

Using (3), (4), (7), (8), (12) the integrated model based on (2) can be obtained.

III. TRAJECTORY TRACKING

In this section, we consider the trajectory tracking of the robotic fish. The equations of motion of the fish are developed in terms of fish CM velocities/accelerations, fish angular velocity/acceleration and the angular angle and acceleration of the fish tail. First, the direct dynamics problem is examined, where the input is the desired motion of the tail and output is the resulting motion of the fish. Then, a method based on the inverse dynamics problem is developed, where the required tail motion is computed in order for the fish to follow a desired trajectory.

A. Direct Dynamics Problem

In accordance to the previous analysis, it can be shown that the direct dynamics problem is described by the fish equations of motion,

$$\dot{v}_{cx} = \frac{m_2}{m_1} v_{cy} \omega_z - \frac{c_1}{m_1} v_{cx} \|\mathbf{v}_c\| + \frac{c_2}{m_1} v_{cy} \|\mathbf{v}_c\| \beta - \frac{c_3}{m_1} \ddot{\theta} \sin(\theta) \quad (13)$$

$$\dot{v}_{cy} = \frac{c_3}{m_2} \ddot{\theta} \cos(\theta) - \frac{m_1}{m_2} v_{cx} \omega_z - \frac{c_1}{m_2} v_{cy} \|\mathbf{v}_c\| - \frac{c_2}{m_2} v_{cx} \|\mathbf{v}_c\| \beta \quad (14)$$

$$\dot{\omega}_z = \frac{m_1 - m_2}{J} v_{cx} v_{cy} - c_4 \omega_z |\omega_z| - c_5 \ddot{\theta} \cos(\theta) - c_6 \ddot{\theta} \quad (15)$$

where the coefficients c_i , $i = 1, \dots, 6$, and the parameters m_1, m_2, J are given in Appendix A.

Equations (13)-(15), define the direct dynamics problem concerning the robotic fish. This means that, for a known motion of the tail, characterized by the tail angle $\theta(t)$ and its angular acceleration $\ddot{\theta}(t)$, (13)-(15) form a system of differential equations which can be solved to yield the corresponding velocities v_{cx} , v_{cy} of the fish, expressed in (\hat{x}, \hat{y}) and its attitude ψ .

Then, using the following transformation between the fish velocities expressed in inertial and body fixed frames, one can derive the resulting motion of the fish, as it is observed in the inertial frame:

$$\begin{aligned} \dot{X} &= \cos \psi \cdot v_{cx} - \sin \psi \cdot v_{cy} \\ \dot{Y} &= \sin \psi \cdot v_{cx} + \cos \psi \cdot v_{cy} \end{aligned} \quad (16)$$

B. Inverse Dynamics Problem

As mentioned above, a more interesting and practical application of (13)-(15), is to derive how the fish tail should move so that the fish executes a desired motion on the plane. This is the inverse dynamics problem. Below we give a universal methodology for any feasible planar curve that a robotic fish is capable of following. Eqs. (13)-(15) are written as:

$$\ddot{\theta} \sin(\theta) = g_1(\dot{v}_{cx}, v_{cx}, v_{cy}, \omega_z) \quad (17)$$

$$\ddot{\theta} \cos(\theta) = g_2(\dot{v}_{cy}, v_{cx}, v_{cy}, \omega_z) \quad (18)$$

$$\ddot{\theta} (c_5 \cdot \cos(\theta) + c_6) = g_3(\dot{\omega}_z, v_{cx}, v_{cy}, \omega_z) \quad (19)$$

where:

$$g_1 = -\frac{m_1}{c_3} \dot{v}_{cx} + \frac{m_2}{c_3} v_{cy} \omega_z - \frac{c_1}{c_3} v_{cx} \|\mathbf{v}_c\| + \frac{c_2}{c_3} v_{cy} \|\mathbf{v}_c\| \beta \quad (20)$$

$$g_2 = \frac{m_2}{c_3} \dot{v}_{cy} + \frac{m_1}{c_3} v_{cx} \omega_z + \frac{c_1}{c_3} v_{cy} \|\mathbf{v}_c\| + \frac{c_2}{c_3} v_{cx} \|\mathbf{v}_c\| \beta \quad (21)$$

$$g_3 = -\dot{\omega}_z + \frac{m_1 - m_2}{J} v_{cx} v_{cy} - c_4 \omega_z |\omega_z| \quad (22)$$

The set of (17)-(19) represents a system of three equations with two unknowns, namely θ and $\ddot{\theta}$. Therefore, the solution of this system must include a compatibility equation. After some algebraic manipulations, (17) and (18), yield the angle and the angular acceleration of the tail, as a function of the linear and angular velocities/accelerations of the fish expressed in (\hat{x}, \hat{y}) as:

$$\theta = \arctan\left(\frac{g_1}{g_2}\right) \quad (23)$$

$$\ddot{\theta} = \pm \sqrt{g_1^2 + g_2^2} \quad (24)$$

Equations (17), (19), and (23) yield an alternative expression for $\ddot{\theta}$, given by:

$$\ddot{\theta} = \frac{g_3 - g_2 c_5}{c_6} \quad (25)$$

Equations (24) and (25) must be fulfilled simultaneously, therefore they impose a compatibility constraint over fish linear/angular velocities and accelerations, as follows:

$$\ddot{\theta} = \frac{g_3 - g_2 c_5}{c_6} = \pm \sqrt{g_1^2 + g_2^2} \quad (26)$$

Considering (16), this constraint results in restrictions on the desired fish trajectory and is the criterion for establishing which trajectories can be implemented. Moreover, the combination of (22) and (26), results in the following differential equation:

$$\dot{\omega}_z = \frac{m_1 - m_2}{J} v_{cx} v_{cy} - c_4 \omega_z |\omega_z| - c_5 g_2 - \text{sgn}(\ddot{\theta}) c_6 \sqrt{g_1^2 + g_2^2} \quad (27)$$

Eq. (27) gives the fish angular acceleration as a function of the fish angular velocity and the linear velocities/accelerations expressed in the body-fixed reference frame. For a desired path in the Cartesian space, given by the velocities $\dot{X}(t), \dot{Y}(t)$ and accelerations $\ddot{X}(t), \ddot{Y}(t)$ of fish CM, the corresponding velocities and accelerations of the fish expressed in the body-fixed frame are given by:

$$\begin{aligned} v_{cx} &= \dot{X} \cos(\psi) + \dot{Y} \sin(\psi) \\ v_{cy} &= \dot{Y} \cos(\psi) - \dot{X} \sin(\psi) \end{aligned} \quad (28)$$

and

$$\begin{aligned} \dot{v}_{cx} &= \ddot{X} \cos(\psi) - \dot{X} \sin(\psi) \dot{\psi} + \ddot{Y} \sin(\psi) + \dot{Y} \cos(\psi) \dot{\psi} \\ \dot{v}_{cy} &= \ddot{Y} \cos(\psi) - \dot{Y} \sin(\psi) \dot{\psi} - \ddot{X} \sin(\psi) - \dot{X} \cos(\psi) \dot{\psi} \end{aligned} \quad (29)$$

Substituting (28) and (29) in (27), one can solve it to find the fish attitude ψ and angular velocity $\omega_z = \dot{\psi}$. Having these variables allows the computation of all other variables of the fish motion. Eq. (23) yields the required tail angle trajectory $\theta(t)$ required to achieve the desired fish motion. Note that solving (27) depends on the sign of the tail angular acceleration. Thus, in order to solve (27), the tail frequency must first be defined. The reason that open-loop control is utilized instead of closed-loop control mode is twofold: (a) the experiments are conducted in a well-controlled environment where external significant disturbances (like waves) are minimal and (b) it is desired for the autonomy and its implementation in the robotic fish. In open sea environments, there is no capability of having cameras over the robotic fish. Moreover, IMUs need constant recalibration and in addition to that the signal of GPS deteriorates in water and makes the periodic surfacing of the robot more than necessary.

IV. IMPLEMENTATION

A. Computation of the Fish Parameters

In order to proceed, one must obtain all the aforementioned coefficients. For this purpose extensive computational fluid dynamics (CFD) simulations were run, using a code which is based on Lattice Boltzmann technology. The main advantage is that through its simple particle based approach, the traditional meshing process, is avoided, reducing significantly the computation time. For simulating robotic fish as two bodies (one main body and one tail which makes an oscillatory motion), moving mesh methods would be needed, which are complex to implement. Instead of solving the Navier Stokes equations, the discrete Boltzmann equation is solved to simulate the flow of a Newtonian fluid with collision models. Thus, we easily simulate a robotic fish in various motions and compute the unknown hydrodynamic coefficients, accepting a small error in our coefficients compared to methods that solve the Navier Stokes equations, such the Finite Element Method (FEM). As mentioned earlier, some hydrodynamic coefficients are variable and related to the fish attack angle. Simplifying the problem, the averages of the variable coefficients are taken over different attack angles. Table I shows the values of the parameters used.

TABLE I
SIMULATION PARAMETERS

Symbol	Quantity	Value	Unit
m_b	Mass of the body	0.3	kg
m^*	Virtual mass	4.42	kg/m
l_1	CM to joint length	0.07	m
l_2	Tail length	0.05	m
J	Inertia of the body	0.0005	kgm ²
S_A	Reference surface area	0.011	m ²
C_D	Drag force coefficient	2.44	-
C_L	Lift force coefficient	3.41	-
K_D	Drag moment coefficient	0.00065	kgm ²
ρ	Density of water	1000	kg/m ³

B. Experimental Set-up & Video Processing

The experimental set-up, used to validate our design, consists of a water tank and a robotic fish. They are both presented in detail in [20]. The dimensions of the robotic fish are 30 cm (L) x 8 cm (W) x 7 cm (H). Due to space limitations, the experimental tank size had to be constrained to 5 m (L) x 1 m (W) x 0.8 m (H). On top of the tank, an overhead camera (Microsoft LifeCam Cinema, 720p, 30fps) is installed. With the help of Matlab and especially with the help of Image Acquisition Toolbox and Image Processing Toolbox, a program was developed that takes as input a top view video of the fish motion and computes off line the obtained fish CM position and velocity as a function of time. The program is based on a Discrete Fourier Transform algorithm (direct and inverse), and it traces the same points through successive images. Through this, we find how certain pixels with the same color or brightness move over time. Besides that, in order to have distinctive points on the fish

body, we mounted three LEDs on the main body, which made possible the localization of the fish main body CM.

V. APPLICATION EXAMPLES

In this section, the direct dynamics problem is validated experimentally and the proposed trajectory tracking methodology, based on the inverse dynamics problem, is confirmed. The planar robotic fish shown in Fig. 2 with its parameters displayed in Table I, is employed. The experiments have been executed using the robotic fish shown in Fig. 1, [20].

The applied tail motion is given by (6) with $\theta_0 = -9.5^\circ$, $A = 15.5^\circ$ and $\omega_t = 2\pi f$, with $f = 1\text{Hz}$. Fig. 3 shows the corresponding experimental and simulated fish trajectories. Note that an approximate 5% error between the experimental trajectory and the Simulated Fish Trajectory 1 exists, and is due to the simplified CFD fish model employed. Using experimental data and identification techniques, a reduced C_D results (i.e. $C_D = 2.074$), which eliminates such error, see Simulated Fish Trajectory 2. The error is also justified by the fact that our tank has relatively small width. Thus, the caudal fin's motion creates ripples which bounce back when they hit on glass and affect our experiments.

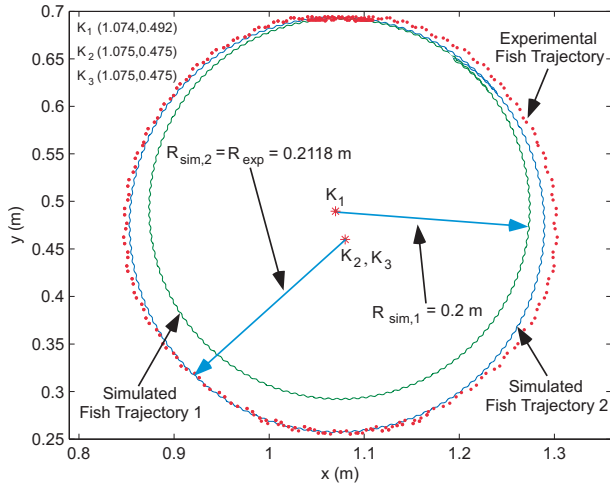


Fig. 3. Direct dynamics problem: The experimental and simulated fish trajectories resulting from a desired tail motion given by (6).

Then, the inverse dynamics problem is considered. In this case, the desired fish trajectory in the Cartesian space is given by the fish CM positions $x(t), y(t)$ shown in Fig. 4 and corresponding to the the simulated trajectory shown in Fig. 3. The desired path satisfies the constraint for the fin acceleration $\ddot{\theta}$, given by (26), therefore it is feasible. For a tail frequency equal to $f = 1\text{Hz}$, the solution of Eq. (27)-(29) yields the necessary fish motion variables (e.g. the fish attitude ψ , the fish angular velocity $\omega_z = \dot{\psi}$ and the surge and sway velocities/accelerations $v_{cx}, v_{cy}, \dot{v}_{cx}, \dot{v}_{cy}$) required to compute the terms g_1, g_2 needed for the estimation of the angle trajectory of the tail, given by (23) and shown in Fig. 5. The resulting signal is an undamped oscillation with $\theta_0 = -9.5^\circ$, $A = 15.5^\circ$ and $\omega_t = 2\pi f$, where $f = 1/T = 1\text{Hz}$, as shown in Fig. 5. A group of snapshots of the robotic fish swimming in a circle is shown in Fig. 6.

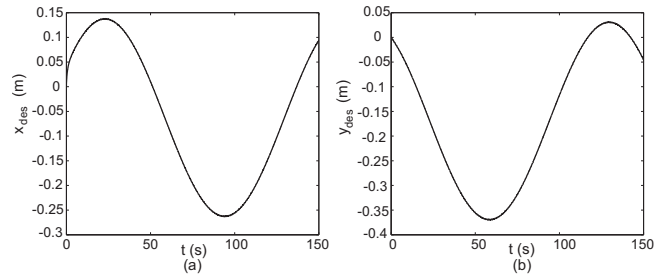


Fig. 4. The desired fish CM trajectory in Cartesian space.

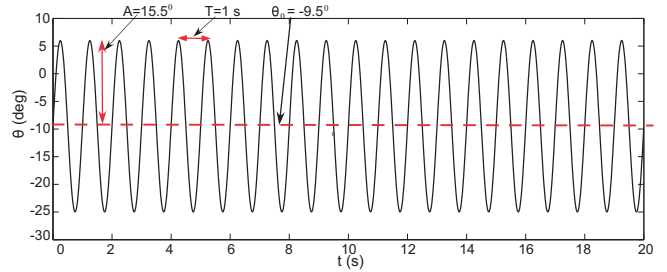


Fig. 5. The required tail motion, resulting from the inverse dynamics problem, in order for the fish to follow the trajectory shown in Fig. 4.

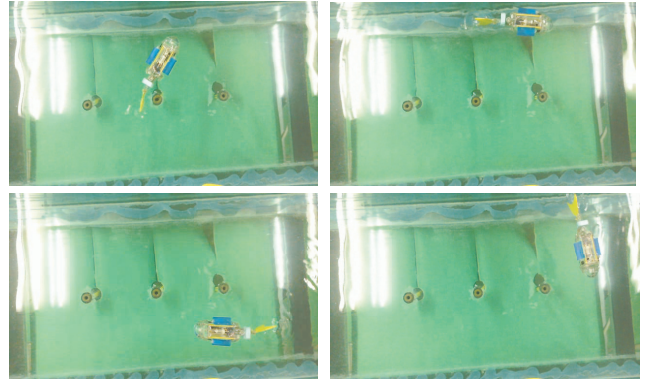


Fig. 6. Snapshots of the CSL robotic fish swimming in a circle.

VI. CONCLUSIONS AND FUTURE WORK

In this paper, a new method for finding how the caudal fin of a robotic fish should move, in order for the fish to follow a given feasible trajectory on the plane, was presented. The conditions, which must be satisfied for the robotic fish to be able to follow a given desired trajectory, were identified. Various simulations were performed and experiments were conducted to validate the model. Simulation results, based on the developed theory, and experimental results were in good agreement.

Future work will be pursued in several directions, so that the small error between theory and experiments is eliminated. Firstly, the various hydrodynamical coefficients will be estimated experimentally with the help of a force/torque sensor. It is expected that more accurate added mass coefficients will be obtained compared to the CFD estimates presented here. Secondly, the experiments will be executed in a larger tank, to eliminate water bouncing off at the side walls of

the water tank and coming back, as this oscillation affects our experimental data. Lastly, we intend to examine the introduction of closed-loop control laws. We strongly believe that with the aforementioned steps, a more accurate tracking response will be obtained.

APPENDIX

The coefficients in (13)-(15) are given by:

$$c_1 = 0.5\rho S_A C_D \quad (30)$$

$$c_2 = 0.5\rho S_A C_L \quad (31)$$

$$c_3 = 0.5m^*l_2^2 \quad (32)$$

$$c_4 = \frac{K_D}{J} \quad (33)$$

$$c_5 = \frac{l_2^2 m^* l_1}{2J} \quad (34)$$

$$c_6 = \frac{m^* l_2^3}{3J} \quad (35)$$

$$m_1 = (m_b - X_{\dot{v}_{cx}}) \quad (36)$$

$$m_2 = (m_b - Y_{\dot{v}_{cy}}) \quad (37)$$

$$J = (I_c - N_{\dot{\omega}_z}) \quad (38)$$

All variables are defined in Table I.

REFERENCES

- [1] EunJung Kim and Youngil Youm. "Design and dynamic analysis of fish robot: PoTuna". In: *Robotics and Automation, 2004. Proceedings. ICRA '04. 2004 IEEE Int. Conf. on.* Vol. 5. Apr. 2004, Vol.5, pp.4887–4892.
- [2] C. Liu et al. "On the shortest path planning for the carangiform robotic fish". In: *Proceedings of the 33rd Chinese Control Conference.* July 2014, pp. 7835–7840.
- [3] H. Kim, B. Lee, and R. Kim. "A Study on the Motion Mechanism of Articulated Fish Robot". In: *2007 International Conference on Mechatronics and Automation.* Aug. 2007, pp. 485–490.
- [4] P. Suebsaiprom and C. L. Lin. "Nonlinear Hinfinity; Guidance and Control for Fish-Robot". In: *11th IEEE Int. Conference on Control Automation (ICCA).* June 2014, pp. 821–825.
- [5] A. R. Chowdhury et al. "Inverse dynamics control of a bio-inspired robotic-fish underwater vehicle propulsion based on Lighthill slender body theory". In: *OCEANS 2014 - TAIPEI.* Apr. 2014, pp. 1–6.
- [6] A. Roy Chowdhury et al. "Kinematics study and implementation of a biomimetic robotic-fish underwater vehicle based on Lighthill slender body model". In: *2012 IEEE/OES Autonomous Underwater Vehicles (AUV).* Sept. 2012, pp. 1–6.
- [7] L. Wen et al. "Novel Method for the Modeling and Control Investigation of Efficient Swimming for Robotic Fish". In: *IEEE Transactions on Industrial Electronics* 59.8 (Aug. 2012), pp. 3176–3188. ISSN: 0278-0046.
- [8] J. Cochran et al. "Source Seeking for Two Nonholonomic Models of Fish Locomotion". In: *IEEE Transactions on Robotics* 25.5 (Oct. 2009), pp. 1166–1176.
- [9] Y. Jia, G. Xie, and L. Wang. "Path planning for robot fish in water-polo game: Tangent circle method". In: *2011 9th World Congress on Intelligent Control and Automation.* June 2011, pp. 730–735.
- [10] I. Ariyanto, T. Kang, and Y. J. Lee. "Dynamics of a Fish-Like Robot and It's Controller Design". In: *2006 SICE-ICASE Int. Joint Conference.* Oct. 2006, pp. 4297–4301.
- [11] V. Kopman et al. "Dynamic Modeling of a Robotic Fish Propelled by a Compliant Tail". In: *IEEE J. of Oceanic Engineering* 40.1 (Jan. 2015), pp. 209–221.
- [12] A. Roy Chowdhury and S. K. Panda. "Finding answers to biological control methods using modulated patterns: An application to bio-inspired robotic fish". In: *2015 IEEE International Conference on Robotics and Automation (ICRA).* May 2015, pp. 3146–3153.
- [13] A. R. Alamdar, M. R. Dehghani, and A. Alasty. "Modeling of tail dynamic behavior and trajectory control of a Fish-Robot using fuzzy logic". In: *2010 IEEE Int. Conference on Robotics and Biomimetics.* Dec. 2010, pp. 885–890.
- [14] P. Luan Nguyen, B. R. Lee, and K. K. Ahn. "Modeling and controlling the descent operation of a fish robot using neural networks". In: *2015 15th Int. Conference on Control, Automation and Systems (ICCAS).* Oct. 2015, pp. 1920–1923.
- [15] Thor I. Fossen. *Guidance and Control of Ocean Vehicles.* 1st Edition. Wiley, 1994.
- [16] J. Wang and X. Tan. "Averaging Tail-Actuated Robotic Fish Dynamics Through Force and Moment Scaling". In: *IEEE Transactions on Robotics* 31.4 (Aug. 2015), pp. 906–917.
- [17] S. B. Behbahani, J. Wang, and X. Tan. "A dynamic model for robotic fish with flexible pectoral fins". In: *2013 IEEE/ASME Int. Conference on Advanced Intelligent Mechatronics.* July 2013, pp. 1552–1557.
- [18] M. J. Lighthill. "Large-Amplitude Elongated-Body Theory of Fish Locomotion". In: *Proceedings Biological Sciences* 179 (1055 Nov. 1971).
- [19] J. Wang, F. Alequin-Ramos, and X. Tan. "Dynamic modeling of robotic fish and its experimental validation". In: *2011 IEEE/RSJ Int. Conference on Intelligent Robots and Systems.* Sept. 2011, pp. 588–594.
- [20] M. Makrodimitris, I. Aliprantis, and E. Papadopoulos. "Design and implementation of a low cost, pump-based, depth control of a small robotic fish". In: *2014 IEEE/RSJ Int. Conference on Intelligent Robots and Systems.* Sept. 2014, pp. 1127–1132.